ISSN 1392–1207. MECHANIKA. 2016 Volume 22(4): 291–296

Research of the friction stir welding process of aluminium alloys

R. Česnavičius*, S. Kilikevičius, P. Krasauskas***, R. Dundulis****, H. Olišauskas*******
**Kaunas University of Technology, Studentų 56, 51424 Kaunas, Lithuania, E-mail: ramunas.cesnavicius@ktu.lt*
***Kaunas University of Technology, Studentų 56, 51424 Kaunas, Lithuania, E-mail: sigitas.kilikevicius@ktu.lt*
****Kaunas University of Technology, Studentų 56, 51424 Kaunas, Lithuania, E-mail: povilas.krasauskas@ktu.lt*
*****Kaunas University of Technology, Studentų 56, 51424 Kaunas, Lithuania, E-mail: romualdas.dundulis@ktu.lt*
*****Kaunas University of Technology, Studentų 56, 51424 Kaunas, Lithuania, E-mail: harius.olisauskas@ktu.edu*

crossref http://dx.doi.org/10.5755/j01.mech.22.4.16167

1. Introduction

It is well known that welding of aluminium alloys using conventional welding methods is a highly costly process, therefore, in order to replace this welding technology, various other joining methods are used. One of them is friction stir welding considered as a non-traditional welding method. This method now is accepted as a standard welding method for aluminium alloys and is used in various fields of industry: aviation, train and marine building, chemical industry etc. to weld aluminium materials which are difficult to weld by other processes [1]. It has the benefits of operation and investment cost savings, weight reduction, high repeatability and consistence, low maintenance, better work environment and recyclability versus other aluminium spot joining methods such as resistance spot welding (RSW) and riveting [2, 3]. This welding method is relative simply, do not requires consumables or filler metal and gas shielding, is low energy consuming process, however needs special welding tool and powerful fixtures to clamp the workpiece. Main parameters which have to be controlled during the process are welding speed and feed which depends on the welding material and the thickness of the welding parts, so to ensure microstructural stability, these processing parameters must be investigated thoroughly [4].

Due to wide applicability, this process is being studied thoroughly. The basic principles of FSW, the weld microstructure and hardness, mechanical properties, including consideration of residual stress, fracture, fatigue and corrosion is described in [5] and is demonstrated that FSW of aluminium has commercial applications.

Friction stir weldability of the 2017-T351 aluminium alloy was investigated in [6], weldability and modelling of the 6061-T6 aluminium alloy in [7], mechanical properties of AA 6082 aluminium alloy butt joints welded by cylindrical taper pin profile in [8], effect of welding speed and tool pin profile on welding zone formation in AA6061 aluminium alloy was investigated in [9].

The overview showed that for different aluminium materials there is no common welding parameters, i.e. for each one's strength, hardness and microstructure should be defined experimentally.

The numerical modelling of the FSW process is a complicated task highly dependent on various factors such as material properties, welding process conditions, geometrical parameters of the tool, etc. During this process, high stress and strain rate takes place and this leads to non-linear material behaviour, excessive mesh distortion and the need for high computational resources; therefore, a modelling of the FSW process for each new case is complicated and specific.

Most of the researches dealing with the topic is focused on the microstructural changes, heat transfer and thermal analysis in FSW. Several approaches are used for modelling the FSW process. Coupled thermo-mechanical modelling is analysed in papers [10-13].

Development of numerical simulation model for FSW employing particle method is presented in [14]. A smoothed particle hydrodynamics (SPH) model for FSW is proposed in paper [15].

Another approach for FSW modelling is the computational fluid dynamics method [16, 17]. However, it is difficult to estimate metal properties of the plastic deformation behaviour applying fluid models for FSW.

This paper presents an experimental investigation and a numerical modelling of the FSW process in order to analyse the influence of different welding parameters on the horizontal welding force.

2. Experimental set-up and results

The FSW experiment was carried out on aluminium alloy AW 10-50 and TL091T4 (AlMg5Mn) 100x50 mm plates with 1.5 mm in thickness using an FSW tool with a special square pin. The shape and dimensions of the FSW tool are shown in Fig. 1. The tool consists of three parts: a shoulder *1* which is made of hot-work tool steel X37CrMoV5-1 EN ISO 4957:2002 and hardened to 50 HRC with a body diameter of 11 mm and a concavity of 5°, a 1.3 mm length square cross-section 3x3 mm tungsten carbide pin *2*, and a M6 screw *3* for fixing pin in the shoulder.

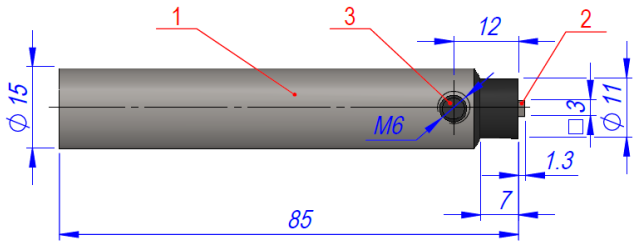

Fig. 1 Common view of the FSW tool with dimensions: *1* - shoulder; *2* - pin; *3* - screw for fixing pin in the shoulder

The experimental setup is shown in Fig. 2. The experiments were carried out on a CNC machining centre "LEADWELL V-20" *1* with a "Fanuc 18*i*-MB" controller

and "Manual Guide *i*" software. The horizontal welding force was measured using a universal laboratory charge amplifier Kistler type 5018A *2* and a press force sensor Kistler type 9345B *3* mounted on the CNC table. Measuring ranges for force of the sensor -10…10 kN, sensitivity: ≈-3.7 pC/N. The amplifier converts the charge signal from the piezoelectric pressure sensor into a proportional output voltage. The variation of the horizontal welding force was recorded to a personal computer *4* using a "PICOSCOPE 4424" oscilloscope *5* and "PicoScope 6" software.

Fig. 2 Experimental setup of the friction stir welding experiments: *1* – machining centre LEADWELL V-20; *2* – "Kistler" amplifier; *3* – "Kistler" force sensor; *4* – computer; *5* – oscilloscope

The tool was plunged into the joining zone of the workpieces by 1.3 mm (in vertical direction) and then welding was performed in horizontal direction. Spindle speeds of 2000, 3000 and 4000 rpm were used and for each of them three tool feed rates of 100, 200 and 300 mm/min were assigned in order to investigate the influence of these parameters on the horizontal welding force magnitude. The results of the investigation of friction stir welding under different spindle speed and feed rates are presented in Table 1.

Table 1

Matrix of the friction stir welding experiments and results

Material	Plates thickness, mm	Spindle speed, rpm	Horizontal feed rate, mm/min	Maximal welding force, N
AW 10-50	1.5	2000	100	2349
		2000	200	2555
		2000	300	2690
		3000	100	2158
		3000	200	2385
		3000	300	2611
		4000	100	2063
		4000	200	2334
		4000	300	2547
TL091T4	1.5	2000	100	1950
		2000	200	1963
		2000	300	1991
		3000	100	1914
		3000	200	1948
		3000	300	1985
		4000	100	1857
		4000	200	1873

An example of AW 10-50 aluminium alloy welded plates at spindle speed of 2000 rpm and feed rate of 100 mm/min is shown in Fig. 3.

Fig 3. AW 10-50 aluminium alloy welded plates at spindle speed of 2000 rpm and feed rate of 100 mm/min

The experiments showed that the horizontal welding force increases as feed rate increases, also the horizontal welding force decreases when the spindle speed increases.

3. Mathematical background of FSW modelling

The governing equation describing the heat transfer during FSW can be expressed as follows [18]:

$$\rho c \frac{\partial T}{\partial t} = \frac{\partial}{\partial x}\left[k_x \frac{\partial T}{\partial x}\right] + \frac{\partial}{\partial y}\left[k_y \frac{\partial T}{\partial y}\right] + \frac{\partial}{\partial z}\left[k_z \frac{\partial T}{\partial z}\right] + G \,, \quad (1)$$

where ρ is the material density; c is the specific heat, T is the temperature, t is the time, k is the heat conductivity, G is the heat generation. Generally, the main heat generation source in FSW is considered to be the friction between the rotating tool and the workpieces and the plastic straining in vicinity of the tool.

For the modelling based on the finite element method (FEM), the Johnson-Cook model was used [19]:

$$\bar{\sigma} = \left(A + B\left(\bar{\varepsilon}_{pl}\right)^n\right)\left[1 + C\, ln\frac{\dot{\bar{\varepsilon}}_{pl}}{\dot{\varepsilon}_0}\right]\left(1 - \left(\frac{T - T_{room}}{T_{melt} - T_{room}}\right)^m\right), \quad (2)$$

where parameter A is the initial yield strength of the material at room temperature, B is the hardening modulus; C is the parameter representing strain rate sensitivity; $\bar{\varepsilon}_{pl}$ is the effective plastic strain; $\dot{\bar{\varepsilon}}_{pl}$ is the effective plastic strain rate $\dot{\varepsilon}_0$ is the reference strain rate; n is the strain hardening exponent; m is the parameter which evaluates thermal softening effect, T_{melt} and T_{room} are the material melting and room temperatures.

4. Computational model for the FSW process

ABAQUS/EXPLICIT software was used for a FEM modelling of the FSW process. The workpieces were created as 10x25x1.5 mm plates. Only these elements of the tool were modelled which can be in contact with the workpieces, besides, the tool model was simplified making the pin round, in order to achieve convergence (Fig. 4).

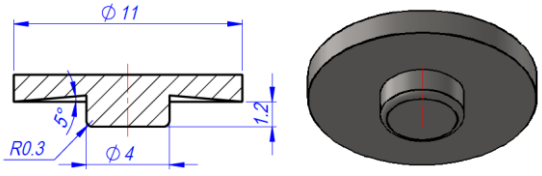

Fig. 4 Dimensions and 3D model of the tool

The adaptive meshing technique was applied by carrying it out for every ten increments and performing five mesh sweeps per adaptive mesh increment. The tool was meshed using element type C3D10MT due to its complex shape and the plates were meshed using element type C3D8RT. An element size of 0.3 mm was used for the tool and an element size of 0.15 mm was used for the plates. 8 layers of elements through the thickness were generated in each of the plates. The mesh of each plate contained 63756 elements while the mesh of the tool contained 55040 elements.

In order to save computational time, the mass scaling technique was used that modifies the densities of the materials in the model and improves the computational efficiency [20], obtaining a stable time increment of at least 0.0001 s step time.

It was assumed that 100% of dissipated energy caused by friction between the parts was converted to heat. The temperature dependent friction coefficient μ of aluminium and steel used in this study is presented in Table 2 [21]. The friction coefficient was set to 0 at the melting temperature of aluminium alloy AW1050.

Table 2

Temperature dependent friction coefficient of aluminium and steel

Temperature (K)	Friction coefficient
273.0	0.610
307.7	0.545
366.3	0.359
420.5	0.255
483.6	0.244
533.0	0.147
588.6	0.135
644.1	0.02
699.7	0.007

Material properties and the Johnson-Cook parameters for aluminium alloy AW 1050 used for the FSW modelling are presented in Table 3 [22].

Table 3

Mechanical properties and the Johnson-Cook parameters for aluminium alloy AW 1050

Parameter	Units	Value
Young modulus, E	GPa	69
Poisson's ratio, ν	-	0.33
Density, ρ	kg/m^3	2710
Melting temperature, θ_{melt}	K	918
Specific heat capacity	J/(kgK)	899
Thermal conductivity	W/(mK)	160
Initial yield strength A	MPa	110
Hardening modulus B	MPa	150
Strain hardening exponent n	-	0.36
Thermal softening exponent m	-	1
Strain rate constant C	-	0.014

The boundary conditions (Fig. 5) were set as follow: the bottom surface and all outer sides of the plates were restrained in all degree of freedom; the top surfaces were under free convection with the convection coefficient of 30 W/m^{2}K; the ambient air temperature and the initial temperature of the workpieces were set to 293 K.

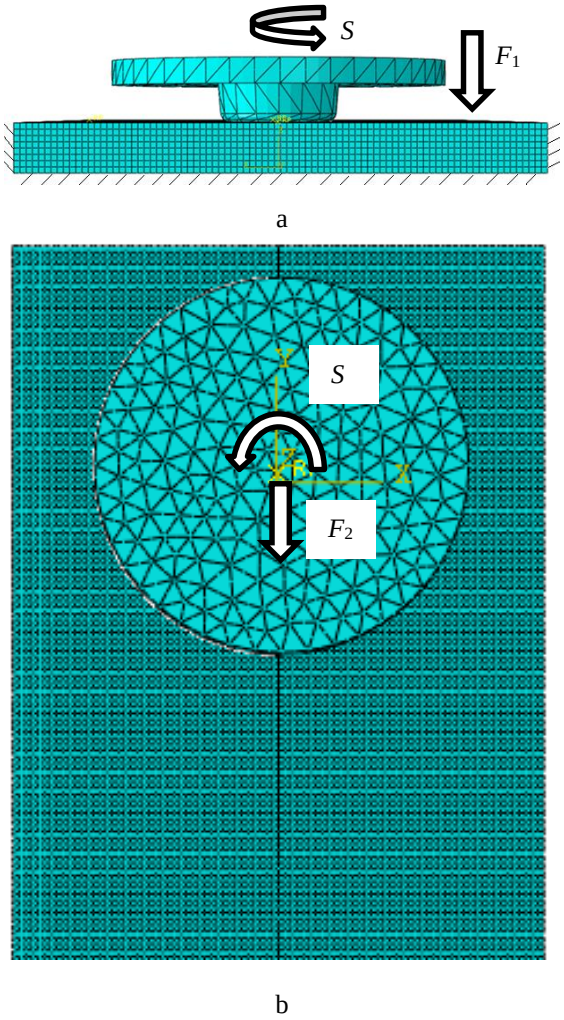

Fig. 5 Mesh and boundary conditions: a - front view during the plunge phase; b - top view during welding

5. Numerical modelling and comparison to the experimental results

Fig. 6 shows how the temperature changes during the FSW process under spindle speed S = 3000 rpm and feed rate F_2 = 300 mm/min. The maximum value was 627 K and it was observed during the tool plunging phase. During the welding, the maximum temperature value was varying between 578 K and 597 K.

Fig. 7 shows the von Mises stress at various instances of time, due to the thermomechanical action. During the plunging phase, when the temperature was 627 K, the maximum value of von Mises stress was about 211 MPa. Under the temperature value of 597 K, the maximum von Mises stress is about 184 MPa.

Fig. 8 shows how the equivalent plastic strain changes during the FSW process. Throughout the whole process, the maximum value of equivalent plastic strain was 0.799.

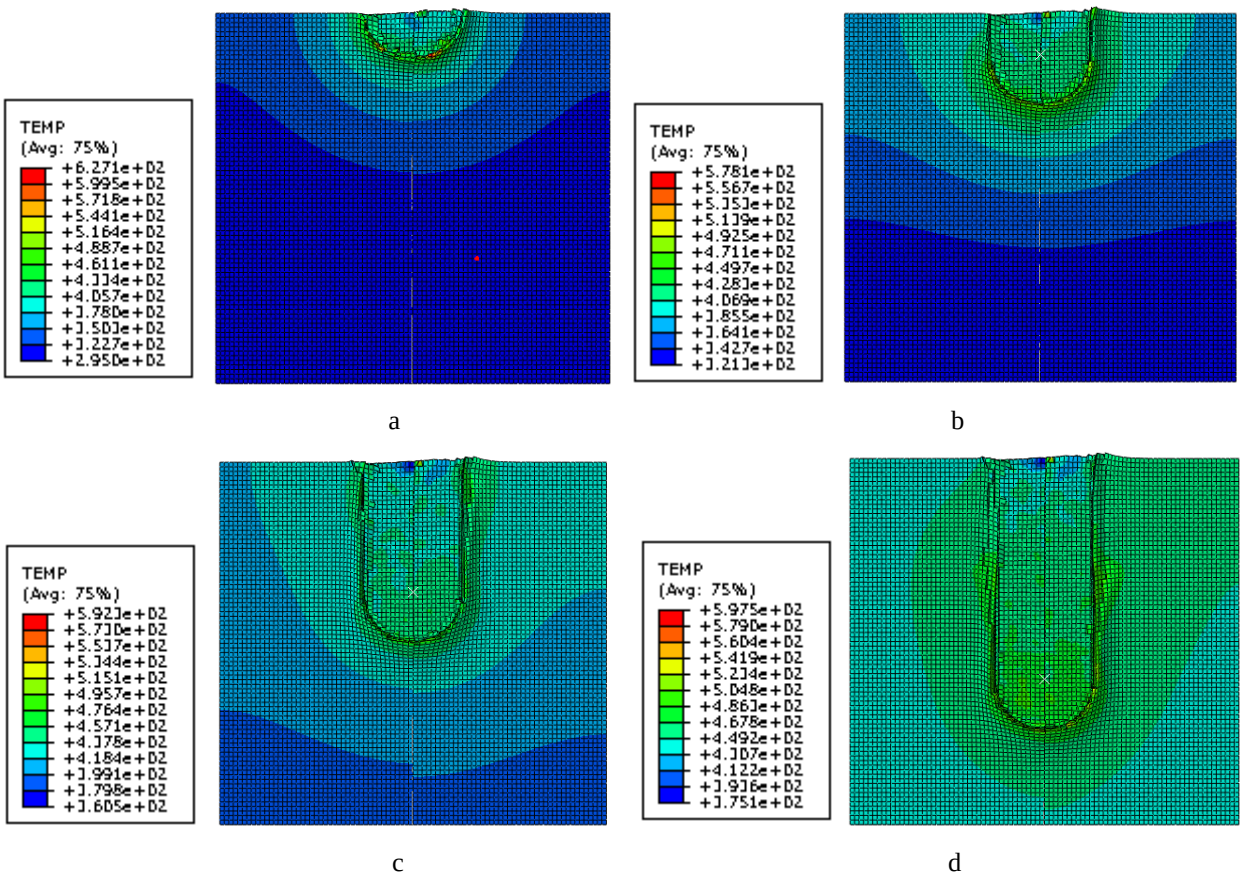

Fig. 6 Temperature (units are in K) at various distances of tool travel: a – 0.5 s; b - 1 s; c - 2 s; d - 3 s; S = 3000 rpm F_2 = 300 mm/min

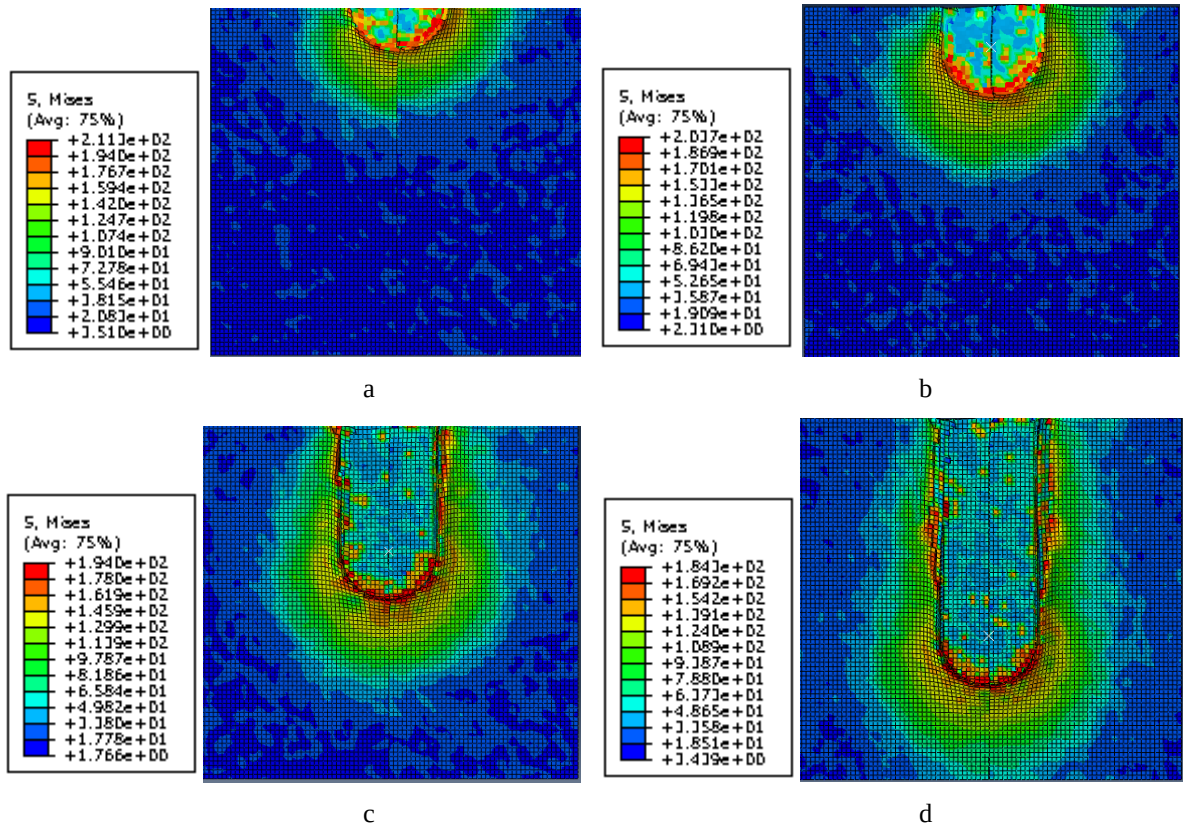

Fig. 7 Von Mises stress at various instances of time: a - 0.5 s; b - 1 s; c - 2 s; d - 3 s; S = 3000 rpm, F_2 = 300 mm/min

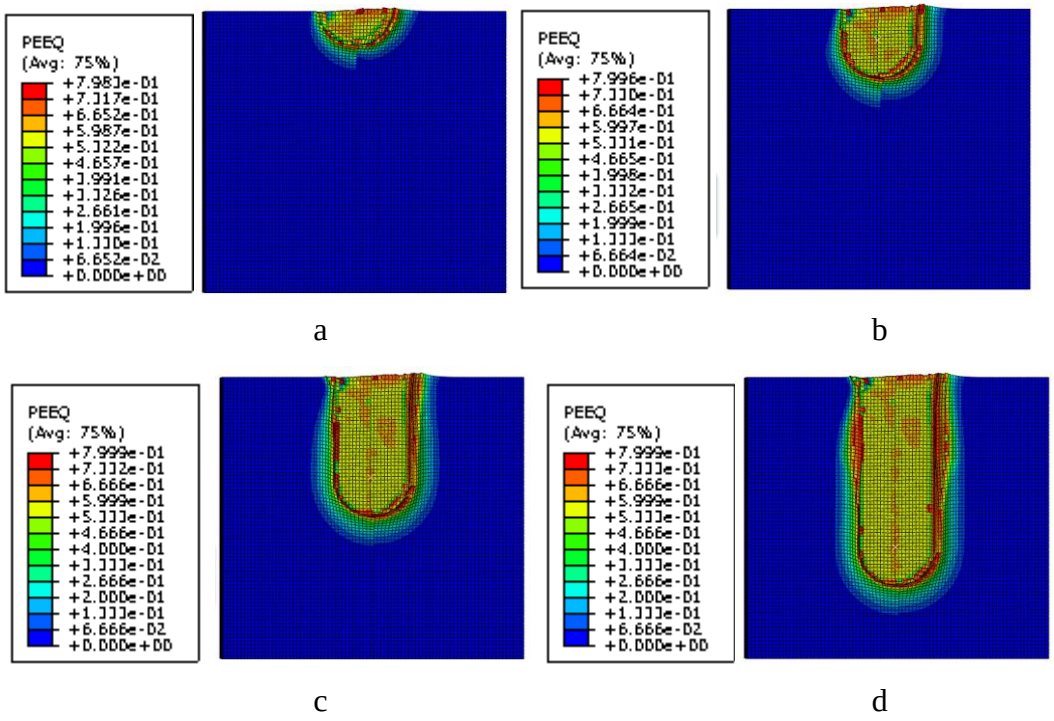

Fig. 8 Equivalent plastic strain at various instances of time: a - 0.5 s; b - 1 s; c - 2 s; d - 3 s; S = 3000 rpm, F_2 = 300 mm/min

The variation of the experimental and the simulated horizontal welding force over time is presented in Fig. 9. The results showed a good agreement in the time intervals between 0 and 1 s and between 2 s and 3 s. In the time interval between 1 s and 2 s the difference was more significant.

However, the trends of the experimental and the simulated welding force variation over time are quite similar and this shows that the presumptions taken in the modelling are quite reasonable.

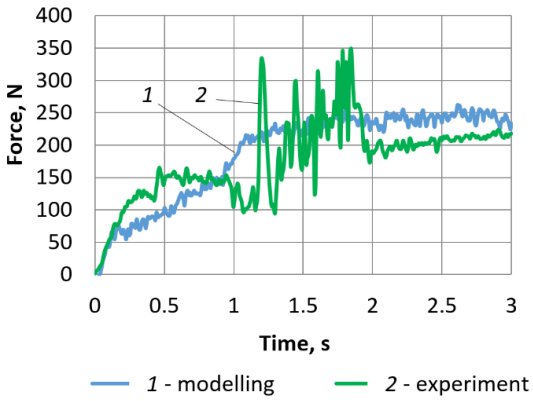

Fig. 9 Variation of the experimental and the simulated welding force

6. Conclusions

An experimental analysis and a numerical modelling of the FSW process were carried out welding two plates of aluminium alloy AW 1050 and TL091T4.

The experiments showed that the horizontal welding force increases as feed rate increases, also the horizontal welding force decreases when the spindle speed increases.

The modelling showed that under spindle speed S = 3000 rpm and feed rate F_2 = 300 mm/min, the maximum temperature value was 627 K and it was observed during the tool plunging phase. During the welding, the maximum temperature value was varying between 578 K and 597 K. During the plunging phase, when the temperature was 627 K, the maximum value of von Mises stress was about 211 MPa. Under the temperature value of 597 K, the maximum von Mises stress is about 184 MPa. Throughout the whole process, the maximum value of equivalent plastic strain was 0.799. A comparison between the experimental and the modelled horizontal welding force showed a good agreement.

The results of the study showed that the presumptions taken in the modelling are reasonable, therefore, the FEM modelling could be used for prediction of rational FSW parameters in order to define lower weld force, which leads to a decrease of tool wear.

References

1. **Smith, C.B.; Hinrichs, J.F.; RuehlFriction, P.C.** Friction Stir and Friction Stir Spot Welding - Lean, Mean and Green. Stir Link, Inc. W227 N546 Westmound Dr., Waukesha, WI 53186.
2. **Pan, T.** 2007. Friction Stir Spot Welding (FSSW) - A Literature Review. SAE 2007 Technical Paper 2007-01-1702. http://dx.doi.org/10.4271/2007-01-1702.
3. **Shibayanagi, T.; Mizushima, K.; Yoshjikawa, S.; Ikeuchi, K.** 2011. Friction stir spot welding of pure aluminum sheet in view of high temperature deformation, Transactions of JWRI 40(2): 1-5.
4. **Yadava, M.K.; Mishra, R.S.; Chen, Y.L.; Carlson, B.; Grant, G.J.** 2010. Study of friction stir joining of thin aluminium sheets in lap joint configuration, Science and Technology of Welding and Joining 15: 70-75.

http://dx.doi.org/10.1179/136217109X1253714565873 3.
5. **Threadgill, P.L.; Leonard, A.J.; Shercliff, H.R.; Withers, P.J**. 2009. Friction stir welding of aluminum alloys, International Materials Reviews 54(2): 49-93. http://dx.doi.org/10.1179/174328009X411136.
6. **Mishra, R.S.; Ma, Z.Y.** 2005. Friction stir welding and processing, Materials Science and Engineering: R: Reports 50(1-2): 1-78. http://dx.doi.org/10.1016/j.mser.2005.07.001.
7. **Zhang, J.; Shen, Y.; Li, B.; Xu, H.; Yao, X.; Kuang, B.; Gao, J.** 2014. Numerical simulation and experimental investigation on friction stir welding of 6061-T6 aluminum alloy, Materials and Design 60: 94-101. http://dx.doi.org/10.1016/j.matdes.2014.03.043.
8. **Srinivasulu, P.; Krishna Mohan Rao, G.; Gupta, MSN.** 2015. Experimental investigation of. mechanical properties of friction stir welded AA 6082 aluminum alloy butt joints, International Journal of Science, Technology & Management 04, Special Issue No. 01: 815-822.
9. **Lakshminarayanan, A.K.; Balasubramanian, V.; Elangovan, K.** 2009. Effect of welding processes on tensile properties of AA6061 aluminium alloy joints, The International Journal of Advanced Manufacturing Technology 40(3): 286-296. http://dx.doi.org/10.1007/s00170-007-1325-0.
10. **Jorge Jr.A.M.; Balancín, O.** 2005. Prediction of steel flow stresses under hot working conditions, Materials Research 8(3): 309-315. http://dx.doi.org/10.1590/S1516-14392005000300015.
11. **Zhu, X.K.; Chao, Y.J.** 2004. Numerical simulation of transient temperature and residual stresses in friction stir welding of 304L stainless steel, Journal of Materials Processing Technology 146(2): 263-272. http://dx.doi.org/10.1016/j.jmatprotec.2003.10.025.
12. **Simões, F.; Rodrigues, D.M.** 2014. Material flow and thermo-mechanical conditions during friction stir welding of polymers: literature review, experimental results and empirical analysis, Materials & Design 59: 344-351. http://dx.doi.org/10.1016/j.matdes.2013.12.038.
13. **Sabooni, S.; Karimzadeh, F.; Enayati, M.H.; Ngan, A.H.W.** 2015. Friction-stir welding of ultrafine grained austenitic 304L stainless steel produced by martensitic thermomechanical processing, Materials & Design 76: 130-140. http://dx.doi.org/10.1016/j.matdes.2015.03.052.
14. **Yoshikawa, G.; Miyasaka, F.; Hirata, Y.; Katayama, Y.; Fuse, T.** 2012. Development of numerical simulation model for FSW employing particle method, Science and Technology of Welding and Joining 17(4): 255-263. http://dx.doi.org/10.1179/1362171811Y.0000000099.
15. **Pan, W.; Li, D.; Tartakovsky, A.M.; Ahzi, S.; Khraisheh, M.; Khaleel, M.** 2013. A new smoothed particle hydrodynamics non-Newtonian model for friction stir welding: Process modeling and simulation of microstructure evolution in a magnesium alloy, International Journal of Plasticity 48: 189-204.
16. **Subrata P., Phaniraj M.P.** 2015. Determination of heat partition between tool and workpiece during FSW of SS304 using 3D CFD modelling, Journal of Materials Processing Technology 222: 280-286. http://dx.doi.org/10.1016/j.ijplas.2013.02.013.
17. **Aljoaba, S. Z.; et al.** 2009. Modeling of friction stir processing using 3D CFD analysis, International Journal of Material Forming 2(1): 315-318. http://dx.doi.org/10.1007/s12289-009-0662-y.
18. **Sathiya, P.; Siva Shanmugam, N.; Ramesh, T.; Murugavel, R.** 2008. Temperature distribution modelling of friction stir spot welding of AA 6061-T6 using finite element technique, Multidiscipline Modelling in Materials and Structures 4(1): 1-14. http://dx.doi.org/10.1163/157361108783470397.
19. **Johnson, G.; Cook, W.** 1983. A constitutive model and data for metals subjected to large strains, high strain rates and high temperatures, Proceeding of the 7th Int. Symp. On Ballistics, The Hague, the Netherlands, p. 1-7.
20. Abaqus Theory Manual, version 6.2, Hibbit, Karlsson & Sorensen, Inc., 2001. p. 841.
21. **Awang, M., et al.** 2005. Thermo-mechanical modeling of friction stir spot welding (FSSW) process: use of an explicit adaptive meshing scheme. SAE 2005 World Congress, Apr., Vol. 13: 1251-1256. http://dx.doi.org/10.4271/2005-01-1251.
22. **Spranghers, K., et al.** 2013. Numerical simulation and experimental validation of the dynamic response of aluminum plates under free air explosions, International Journal of Impact Engineering 54: 83-95. http://dx.doi.org/10.1016/j.ijimpeng.2012.10.014.

R. Česnavičius, S. Kilikevičius, P. Krasauskas,
R. Dundulis, H. Olišauskas

RESEARCH OF THE FRICTION STIR WELDING PROCESS OF ALUMINIUM ALLOYS

S u m m a r y

This paper presents an experimental investigation and a numerical modelling of the friction stir welding (FSW) process on aluminium alloy AW 1050 and TL091T4 plates. The experiments were done in order to analyse the influence of different welding parameters on the horizontal welding force. The modelling of the FSW process of AW 1050 aluminium alloy was carried out and the temperature, von Mises stress, equivalent plastic strain and horizontal welding force variation over time were obtained. A comparison between the experimental and the modelled horizontal welding force showed a good agreement. The obtained results of the presented study lead to a conclusion that the presumptions taken in the modelling are reasonable, therefore, the FEM modelling could be used for prediction of rational FSW parameters in order to define lower weld force, which leads to a decrease of tool wear.

Keywords: friction stir welding, welding force, modelling.

Received April 20, 2016
Accepted July 04, 2016